Journal of Marine Systems 191 (2019) 51–63

Contents lists available at ScienceDirect

Journal of Marine Systems

journal homepage: www.elsevier.com/locate/jmarsys

The influence of environmental factors and hydrodynamics on sardine (*Sardina pilchardus*, Walbaum 1792) abundance in the southern Alboran Sea

A. Jghab[a,b,c], M. Vargas-Yañez[a], A. Reul[b], M.C. Garcia-Martínez[a,*], M. Hidalgo[a], F. Moya[a], M. Bernal[d], M. Ben Omar[e], S. Benchoucha[e], A. Lamtai[e]

[a] Instituto Español de Oceanografía. C.O.Málaga, Spain
[b] Universidad de Málaga, Andalucía Tech, Departamento de Ecología y Geología, Campus de Teatinos s/n, 29071 Málaga, Spain.
[c] Abdelmalek Essaadi University, Morocco.
[d] General Fisheries Commission for the Mediterranean, Rome, Italy.
[e] National Institute for Fisheries Research, Morocco.

ARTICLE INFO

Keywords:
Sardine
Alboran Sea
Environmental factors
Climate change

ABSTRACT

The study of environmental variables and their influence on the small pelagic fish stocks of the Alboran Sea (Western Mediterranean) is asymmetrical, with studies focused on the southern coast being scarce compared with those looking at the northern margin. In this work, time series of sardine landings from the Moroccan coast of the Alboran Sea from 1981 to 2016 were analyzed together with environmental variables such as Sea Surface Temperature (SST), Sea Surface Salinity (SSS), Surface Chlorophyll-a concentrations (Chl-a), and the velocity of the Atlantic Jet (AJ) flowing into the Mediterranean Sea through the Strait of Gibraltar. Annual sardine catches decreased from 1981 to 2016 at a rate of −258 t/year. At the same time, the SST and SSS increased at rates of 0.03 °C/year and 0.004 ups/year, respectively, very likely as a result of climate change. Linear models reflect a negative relationship between sardine landings and SST and SSS, indicating that the long-term temperature and salinity changes in the Mediterranean could have a negative impact on sardine abundance. At an inter-annual time scale, chlorophyll concentrations seem to be positively related to sardine abundances. A decrease in the kinetic energy of the AJ is also inferred from the cross-strait sea level difference (SLD). This variable has an important influence (positive correlation) on sardine landings, both in the long term and at the inter-annual time scale, with higher sardine abundances associated to higher SLD. This work shows that environmental variables such as SLD, SST, SSS, and Chl-a are the main driving factors for the variability of sardine landings in the southern Alboran Sea.

1. Introduction

Small pelagic species are very important in commercial fisheries, making up 22% of global marine catches around the world (FAO, 2011).This is true for the Mediterranean and Black Sea where anchovies (393,500 tons/year) and sardines (186,100 tons/year) are the dominant species, accounting for 26% and 12% of the total catch (FAO, 2016). These species play a key role in marine ecosystems because of their high biomass and their role in linking lower and higher trophic levels (Bakun, 1996). Small pelagic fish with fast growth, early maturation, and few reproductive age classes are highly vulnerable to environmental changes due to their strong dependence on the sub-surface hydro-climatology and the spatial and temporal variability of primary production (Brosset et al., 2015, 2016, 2017; Hidalgo et al., 2011; Lloret et al., 2004). Another factor affecting these species is the increasing fishing effort. Catches are experiencing negative trends suggesting a possible decline of the stocks (GFCM, 2016). Pinsky et al. (2011) demonstrated that the probability of these fisheries collapsing is similar to that observed for large body and late-maturity species.

Climate change is recognized as another potential threat to exploited marine resources (FAO, 2008), with changes in sea temperature potentially altering the biology of marine species, their seasonal cycles, and their distribution. These changes could have a higher impact on small-bodied and fast-growing species, like small pelagic fish (Perry et al., 2005). Because of its reduced dimensions when compared with the world oceans, and its semi-enclosed character, the Mediterranean Sea could be particularly sensitive to climate change (Garcia-Martinez et al., 2018; Vargas-Yáñez et al., 2017; Bethoux et al., 1999).

* Corresponding author.
E-mail address: mcarmen.garcia@ieo.es (M.C. Garcia-Martínez).

https://doi.org/10.1016/j.jmarsys.2018.12.002
Received 28 May 2018; Received in revised form 6 November 2018; Accepted 2 December 2018
Available online 06 December 2018
0924-7963/ © 2018 Elsevier B.V. All rights reserved.

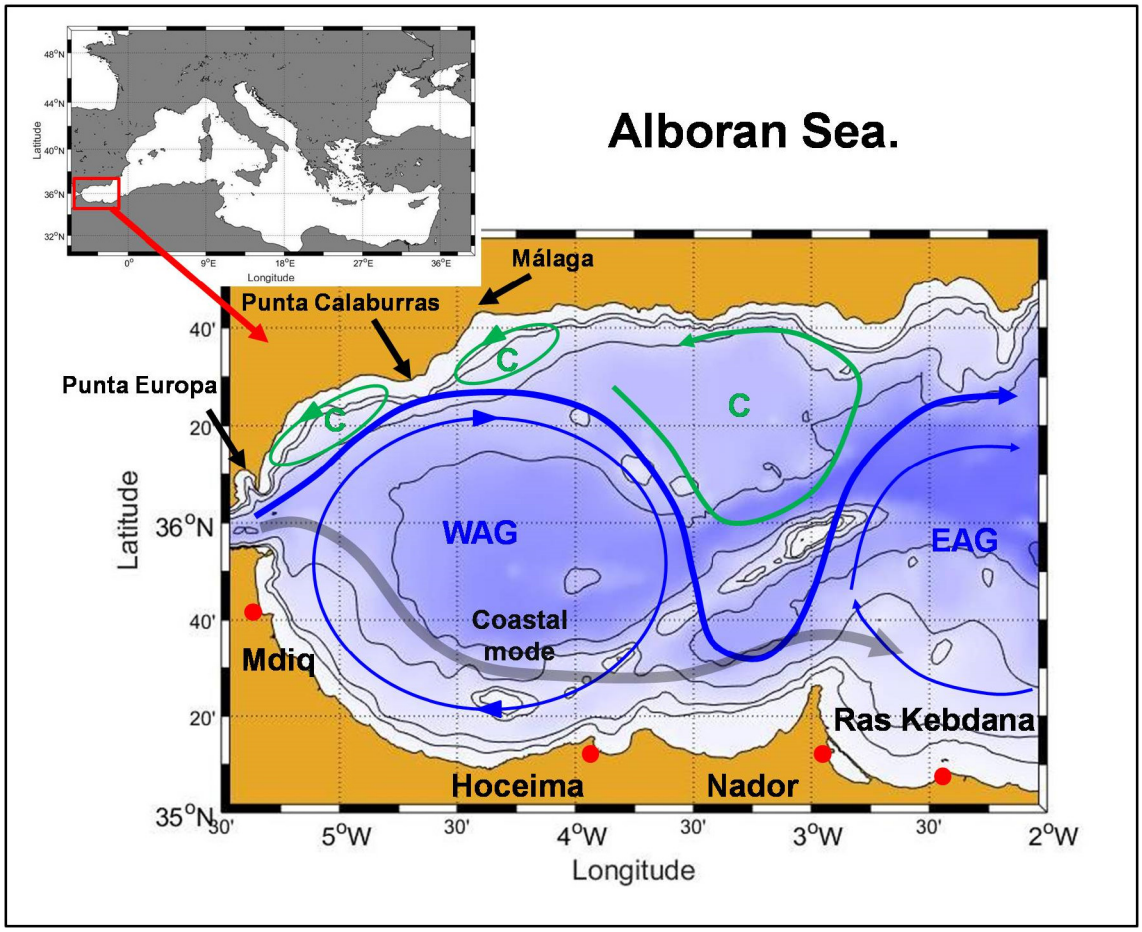

Fig. 1. Alboran Sea map showing the main surface circulation patterns and the main Moroccan ports from where landing data have been obtained (Mdiq, Hoceima, Nador and Ras Kebdana). The blue lines show the most frequent position of the Atlantic Jet (AJ) and the two anticyclonic cells: Western Alboran Gyre (WAG) and Eastern Alboran Gyre (EAG). The grey line shows the AJ when a coastal mode circulation is established. The green lines show the presence of very frequent cyclonic eddies. (For interpretation of the references to color in this figure legend, the reader is referred to the web version of this article.)

The Mediterranean Sea is considered a biodiversity hotspot, but it is also subject to anthropogenic stressors (Coll et al., 2011). Examples of these alterations are presented by Piroddi et al. (2017), who evidenced the effect of changes in primary production and fisheries pressure on the dynamics of fish species in the Mediterranean, where fish stocks have decreased by 34% (both commercial and non-commercial species). Tugores et al. (2011) showed the impact of environmental variables such as temperature, salinity, and chlorophyll concentration on sardine habitat suitability, and Raybaud et al. (2017) suggested that climate change could cause a moderate decrease in anchovy abundance during the 21st century. Brosset et al. (2017) found a decrease in anchovy and sardine body condition, but this could not be related to the main climatic indices. These authors suggested that regional environmental changes and their impact on phyto- and zooplanktonic assemblages could be linked to this body condition decrease through bottom-up control mechanisms (Brosset et al., 2015, 2016). Sabatés et al. (2006, 2009) showed that sea water warming was responsible for the change in the distribution of *Sardinella aurita* which had extended northwards into the North Western Mediterranean Sea (Catalan shelf).

The sardine (*Sardina pilchardus*, Walbaum 1792) is one of the most abundant species in the Mediterranean Sea and is a suitable case study for analyzing the influence of environmental factors on the variability of small pelagic populations. Sardine spawning seems to occur preferentially in the temperature window 13.5–15 °C (Bernal et al., 2007), with the reproductive season changing geographically depending on the period of the year when appropriate water temperatures are reached. In the Mediterranean Sea, sardine larvae are found during the autumn and winter in the Catalan Sea (Olivar et al., 2010; Palomera et al., 2007; Sabatés, 2004; Olivar et al., 2001). Abad and Giráldez (1993) found that maxima in sardine reproductive condition corresponded to December and January. These authors previously observed that changes in the winter temperature could alter the intensity and phenology of the spawning season. Thus, temperature can be considered a key factor modulating sardine reproduction in the Mediterranean Sea, and changes in water temperature caused by climate change should be considered in assessment frameworks/models. Other environmental factors could also have a significant impact on sardine abundance and distribution, including salinity and food abundance. Both sardine larvae and adults prey on micro phyto- and zooplankton, as well as mesozooplankton (Barroeta et al., 2017; Costalago et al., 2012, 2014), and therefore changes in primary and secondary production could affect larval survival as well as the condition of spawners (Brosset et al., 2015, 2016). Sabatés (2004) and Olivar et al. (2001) found that, unlike anchovy larvae, which are concentrated in the top 10 m of the water column, sardine larvae are distributed homogeneously from the surface to a depth of 40 m, coinciding with winter mixing and high productivity in a homogeneous water column. In fact, the reproductive strategy of *Sardina pilchardus* seems to involve energy accumulation during the months prior to reproduction (i.e., it is a capital breeder; Barroeta et al., 2017; Albo-Puigserver et al., 2017; Abad and Giráldez, 1993). Together, these results suggest that an increase in water column stratification caused by surface water warming, or the extension of the stratified period in the Mediterranean Sea, could reduce primary production hence affecting the availability of prey for

sardine larvae and adults. Nevertheless, winter mixing is not the only factor modulating primary production in the Mediterranean. Wind-induced upwelling, mesoscale structures, and thermal and haline fronts should also be considered as potential fertilizing mechanisms at local-regional scales (Sarhan et al., 2000; Ruiz et al., 2001). All these processes occur in the Alboran Sea, which is one of the areas in the Mediterranean Sea with the most intense hydrodynamics and high primary production (Bosc et al., 2004).

The Alboran Sea has complex hydrodynamics, with several upwelling mechanisms fertilizing its waters. It also has a high primary and secondary production (Oguz et al., 2014) compared to other areas in the Mediterranean Sea. All these factors make the Alboran Sea a challenging system in which to investigate the influence of environmental variability on abundance fluctuations in small pelagic fish, such as the sardine. A fast (~1 m/s) current of Atlantic water flows into the Alboran Sea through the Strait of Gibraltar, compensating for the freshwater deficit of the Mediterranean Sea. This Atlantic jet (AJ) surrounds and feeds two anticyclonic gyres in the western and eastern sub-basins of the Alboran Sea (Fig. 1). The geostrophic adjustment of the AJ generates frontal areas with primary production that is higher than that found in other areas of the Mediterranean (Morán and Estrada, 2001; Minas et al., 1991). Cyclonic circulation areas are frequently found to the north of the jet, mainly to the northeast of the Gibraltar Strait and in front of Malaga Bay (Reul et al., 2005). Finally, westerly winds prevail from autumn to the end of spring, causing upwelling events and phytoplankton blooms on the northern coast of the Alboran Sea. This hydrodynamic scheme is far from stationary, and presents a high inter-annual variability. The AJ is very variable, and can shift from the two-gyres mode to a coastal-jet mode where it flows close to the African coast (Vargas-Yáñez et al., 2002). The velocity of the AJ flowing into the Mediterranean Sea through the Strait of Gibraltar could be a key factor in determining this variability (Bormans and Garrett, 1989). The southward displacement of the AJ and the shift from one circulation mode to the other may constitute a further upwelling mechanism (Sarhan et al., 2000). These displacements and the kinetic energy of the jet could also have significant influence on the recruitment success of small pelagic fishes (Ruiz et al., 2013).

Our knowledge of biogeochemical cycles and variability, and primary and secondary production and their link with higher trophic levels on the two sides of the Alboran Sea is asymmetrical. Unlike for the northern Alboran Sea, there is very little work dealing with these issues in the southern sector. One of the few studies looking at the inter-annual variability of small pelagic fishes and environmental variables, describes a significant negative correlation between monthly sardine landings per unit effort (LPUE) in Hoceima port and sea surface temperature (SST) and chlorophyll-a concentrations (Chl-a) (Abdellaoui et al., 2017). However, it is still not known whether this influence is generalized across the whole Alboran Sea and whether other additional environmental drivers may affect the fluctuating dynamics of sardine LPUE. This lack of information on the influence environmental factors have on small pelagic fishes in the southern Alboran Sea is especially relevant if we consider that sardines (9270 tons/year) and anchovies (1033 tons/year) comprise the highest catches along the Mediterranean coast of Morocco (INRH/DRH, 2016).

The goal of this work was to test the influence of various environmental variables on both the long-term and inter-annual variability of sardine catches in the southern part of the Alboran Sea. Multiple linear regression models have been used to identify the main environmental variables correlating with the variability of sardine catches. Based on our model results we discuss the possible mechanistic links relating sardine abundance fluctuations to the hydrodynamic and environmental variability of the Alboran Sea, including a potential link to long-term changes induced by climate change.

2. Data and methods

Data on the monthly sardine landings on the Mediterranean Moroccan coast from 1983 to 2016 were obtained from the Moroccan National Institute of Fisheries. Fig. 1 shows the position of the main ports, Mdiq, Hoceima, Nador, and Ras Kebdana, although some other, smaller ports also contribute to the total sardine landings in this area. The main features of the surface circulation and the main cyclonic and anticyclonic areas are included. The fleet effort (fishing days) was only available from 2009 to 2016. Landings per Unit Effort (LPUE) for this period were estimated as landings in metric tons divided by the number of fishing days.

In addition to sardine landings, information on environmental variables that potentially impact sardine recruitment and abundance were obtained from various sources. These variables are sea surface temperature (SST), sea surface salinity (SSS), surface chlorophyll-a concentration (Chl-a), the west-east (u) and south-north (v) components of the wind, the North Atlantic Oscillation (NAO) index, the Mediterranean Oscillation Index (MOI), and the Western Mediterranean Oscillation index (WeMO). SST, SSS, and Chl-a data were averaged over the southern part of the Alboran Sea, from 5.5°W to 2°W and from 35°N to 36°N.

Daily sea surface temperature data from 1981 to 2017 were obtained from NOAA high-resolution SST data, from the NOAA/OAR/ESRL PSD, Boulder, Colorado, USA web site at https://www.esrl.noaa.gov/psd/ (Reynolds et al., 2007). This data set has a 0.25° × 0.25° resolution. Daily salinity data from 1987 to 2017 were obtained from The Copernicus Marine Environment Monitoring Service (Simoncelli et al., 2014). This dataset has a 0.063° × 0.063° resolution. Daily Chlorophyll-*a* data were also obtained from the Copernicus website. These data have a spatial resolution of 1 km × 1 km and run from 1997 to 2016 (available from GOS-ISAC-CNR, Volpe et al., 2012). Daily wind data with a 2.5° × 2.5° resolution (u, west-east and v, south-north components) were obtained from NCEP Reanalysis, from the NOAA/OAR/ESRL PSD, Boulder, Colorado, USA web site at https://www.esrl.noaa.gov/psd/ (Kalnay et al., 1996).

The AJ in the Gibraltar Strait was considered to be another environmental variable with the potential to impact small pelagic fish. However, long time series for this variable are not available. To circumvent this limitation, and according to García-Lafuente et al. (1998) and Vargas-Yáñez et al. (2002), the AJ can be considered to be in geostrophic equilibrium with the cross-strait sea level difference according to:

$$u = \frac{g\Delta\xi}{fL}$$

where u is the along-strait component of the Atlantic flow velocity, g is the gravity acceleration ($9.8\,\mathrm{ms}^{-2}$), f is the Coriolis parameter at a latitude of 36°N ($8.5 \times 10^{-5}\,\mathrm{s}^{-1}$), L is the cross-strait distance, and $\Delta\xi$ is the sea level difference between Ceuta and Algeciras. According to this expression, the Algeciras-Ceuta sea level difference can be considered a good indicator of the changes in the inflowing velocity. Monthly sea level time series for Algeciras and Ceuta were obtained from the tide gauge network of the Instituto Español de Oceanografía and Permanent Service for Mean Sea Level (www.psmsl.org). Monthly time series for the cross-strait sea level difference were constructed for 1981 to 2016.

Finally, the main atmospheric circulation patterns in the North Atlantic and Mediterranean Sea can influence the productivity of Mediterranean waters, in addition to the distribution and abundance of plankton (García-Comas et al., 2011; Fernández de Puelles et al., 2007) and high trophic level organisms (Hidalgo et al., 2011, 2015). Winter (December to March) and annual NAO indices were obtained from the National Centre for Atmospheric Research (2017). The NAO index is defined as the normalized sea level pressure difference between the Azores and Iceland. The Mediterranean Oscillation Index (MOI) is

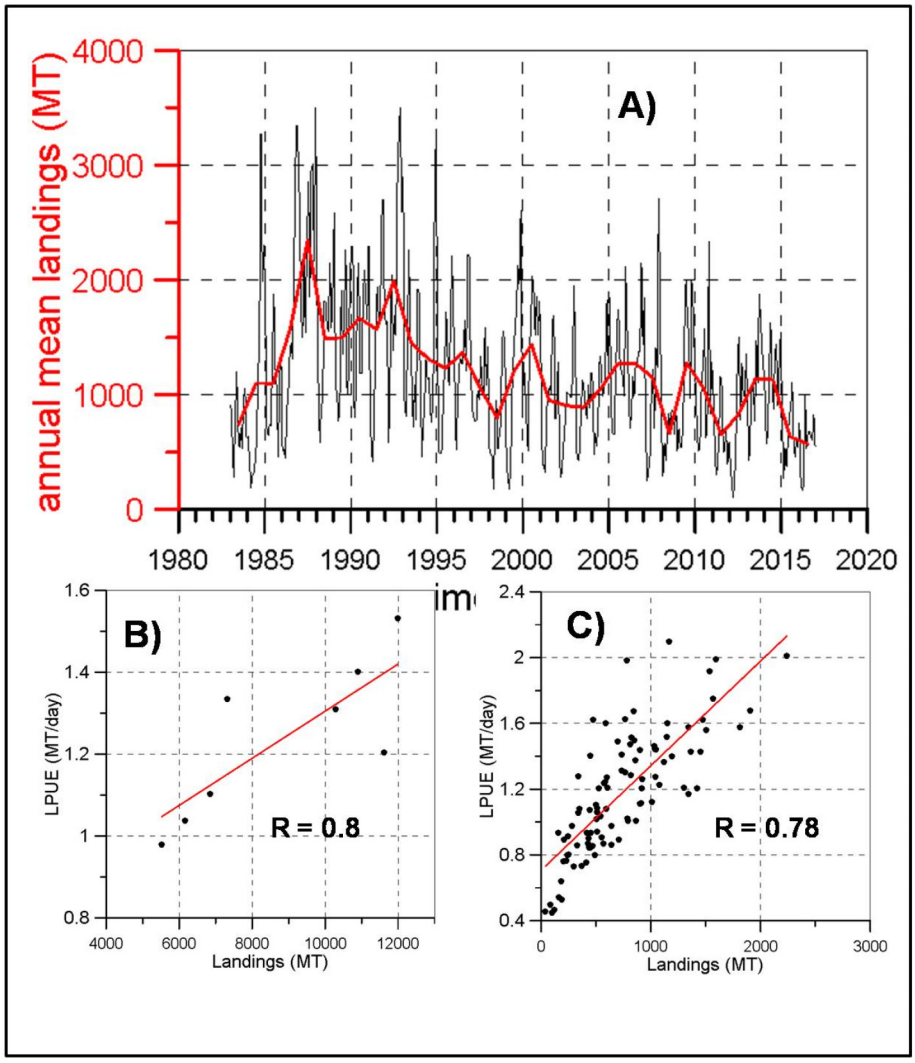

Fig. 2. A) Time series of monthly landings (black line), and mean monthly landings obtained averaging the twelve monthly data for each year (red lines), both expressed in tones. B and C show the linear regression analysis between LPUE and landings for both annual and monthly time series, respectively. The correlation coefficient is included in both plots. (For interpretation of the references to color in this figure legend, the reader is referred to the web version of this article.)

defined as the normalized sea level pressure difference between Gibraltar and Israel. MOI values were obtained from the Climate Research Unit, University of East Anglia. The Western Mediterranean Oscillation index is more local, and defined as the pressure difference between San Fernando, in the Gulf of Cádiz, Spain, and Padua, in northern Italy (Martín-Bide and López-Bustins, 2006). These data were obtained from the Climatology Group at Barcelona University (www.ub.edu/gc/en).

2.1. Time series averaging and EOF analysis

Monthly landings from the Mdiq, Hoceima, Nador, and Ras Kebdana ports were aggregated. The high variability in monthly time series of sardine landings (black line in Fig. 2A) is beyond the scope of this current study. Therefore, the monthly time series were annually averaged, in other words, the twelve monthly values for each year were averaged. In this way, we obtained one data point per year (hereafter mean monthly landings; red line in Fig. 2A). Many studies have shown that LPUE are an appropriate proxy for the abundance of different species. Ruiz et al. (2013) used LPUE to estimate the variability of anchovy abundance in the Alboran Sea, Thiaw et al. (2017) used LPUE as a proxy for the abundance of *Sardinella* along the northwestern African coast, and Massutí et al. (2008) and Hidalgo et al. (2011) used it to analyze European Hake in the Balearic Sea. Nevertheless, fishing effort data for the fleet targeting sardine in Moroccan Alboran waters are only available from 2009 onwards. This considerably reduces the length of the time series analyzed and the possibility of finding meaningful relationships with environmental variables. Using landings instead of LPUE would increase the length of the available time series, but changes in sardine landings could simply be the result of changes in the fishing effort, and not be a reflection of the real variability in the stock abundance. To check this possibility, a regression analysis between landings and LPUE was undertaken for both the annual and monthly time series, which revealed a high and significant correlation in both cases, supporting the use of landings as a response variable (Fig. 2B and C). This result indicates that the abundance variability of sardines in the southern Alboran Sea could be described through sardine landing data. This result coincides with the high level of correlation between landings and LPUE for the northern sector of the Alboran Sea (see for instance, Fig. 28 in Copemed, 2017). This close relationship between landings and LPUE has already been demonstrated for the juvenile sardine landings in Vigo (Atlantic Iberian coast, Guisande et al., 2004) and the port of Tarragona (northwestern Mediterranean, Lloret et al., 2004).

SST, SSS, and surface Chl-a were processed in two different ways. The data were distributed on regular grids at different resolutions, as explained above. In order to describe the fluctuations in the variables directly affecting the southern Alboran Sea, grid points from 5.5° W to

2° W and to the south of 36° N were selected and annually averaged. In this way, annual time series for SST, SSS, and Chl-a were obtained for the southern half of the Alboran Sea.

Directly calculating the mean values for the southern Alboran Sea allows us to analyze the relationships between the sardine landings from this sector and the environmental variables observed in the same geographical area. Nevertheless, the Alboran Sea has highly energetic hydrodynamics. Primary production, or the phyto- and zooplankton distributions, which can affect the fish stocks in certain regions (Brosset et al., 2015, 2016, 2017) could result from advection and other processes occurring in nearby locations. We therefore considered that the variability in the abundance of the sardine stock could also be related to the hydrodynamic structures and circulation patterns in the Alboran Sea, and their influence on variables such as SST, salinity and chlorophyll. Empirical orthogonal functions (EOF) and the time evolution of the associated modes of variability have previously proven to provide further insight into such dynamics and the variability of the hydrographic structures (Parada and Canton, 1998; Garcia-Gorriz and Carr, 2001; Baldacci et al., 2001). Details on the EOF analysis can be seen in the references above or in Preisendorfer (1988). Here we briefly summarize the main ideas.

A time series of SST, SSS, and Chl-a is available for each grid point (latitude/longitude) within the selected geographical area (Alboran Sea). These time series are not statistically independent, and the variability at each grid point can be considered to be the result of variation in several spatial structures. Each of these spatial structures is an EOF. As an example, the upper panels in Fig. 5A and B represent the first and second EOFs for SST. The color scale shows the coefficients, or weights, that the EOF associates to each latitude/longitude. If all the coefficients have the same sign, this indicates that the SST (or the variable analyzed) will change in phase across the entire region. In other words, it will increase or decrease simultaneously at all the grid points. This time variability is expressed by the time series, or mode of variability, associated to each spatial structure and presented in the lower panels of Fig. 5A and B. If the EOF presents sign changes, this indicates that when SST is increasing at some locations, it is decreasing at others. The amplitude of changes at each grid point is the spatial weight (EOF) multiplied by the value of its associated time series.

2.2. Linear trends

Linear trends were estimated by fitting a straight line to all the time series (sardine landings and environmental predictors) by means of least square fit. The slope represents the mean annual rate of change. Confidence intervals at the 95% confidence level were obtained for the slope considering a Student's t-distribution after checking for the normality of the residuals (Kolmogorov-Smirnov tests, see Zar, 1984 for instance). All the calculations involved in the model selection were repeated using both original and detrended time series (see Section 2.3.2). Table 1 shows the slope (a1), ordinate intercept (a0), explained variance (R2), and the probability level (p) for the significant linear trends.

2.3. Linear models and model selection

2.3.1. Exploratory data analysis

Although all the environmental variables described above are based on sound scientific knowledge, the number of predictors used to model the variability of sardine landings should be kept as low as possible, according to the degrees of freedom in the analysis (Burnham and Anderson, 2002). For this reason, a first exploratory analysis of the data was undertaken. Scatter plots of SST, SSS, Chl-a, SLD, and climatic indices (NAO, MOI, WeMO) versus sardine landings were analyzed. The same analysis was carried out for the main variability modes of SST, SSS and Chl-a. Sardine landings were regressed on these variables, and only those significantly correlating at the 0.1 significance level were considered potential predictors for the generation of candidate linear models. Those variables not significantly correlating were discarded. This analysis was considered for the environmental variables already described, with and without a one-year time lag. In addition, the sardine abundance in the previous year may also exert a certain influence over the following year's landings (density-dependent effect). Therefore, sardine landings from the previous year were also considered a potential predictor that could be included in the model as a first order autoregressive term.

Table 1
Linear trends intercept (a_0), slope (a_1), explained variance (R^2) and p level for those variables with statistically significant linear trends.

	a_0	a_1	R^2	p
Sardine	44,232.61	−21.52	0.31	0.00
SST	−38.13	0.03	0.65	0.00
SSS	26.94	0.004	0.32	0.00
Chl-a	−8.33	0.005	0.22	0.04
U	−48.41	0.02	0.18	0.01
V	−25.43	0.01	0.29	0.00
Mode1SST	−452.92	0.23	0.59	0.00
Mode2SST	−84.52	0.04	0.31	0.00
Mode1Sal	−187.10	0.07	0.32	0.00
Mode1Chl a	−214.0	0.11	0.31	0.01
Mode3Chla	−96.0	0.05	0.31	0.01
SLD	3585.66	−1.78	0.43	0.00

2.3.2. Modeling the complete time series

Once the potential predictors had been selected (see Section 2.3.1), the sardine landings $S(t)$ were modeled as:

$$S(t) = \sum_{i=1}^{k} \alpha_i P_i(t) + \sum_{j=0}^{k} \beta_j P_j(t-1) + \varepsilon(t) \quad (1)$$

where t is the time in years, S is the sardine landings, and P_i is the possible predictors: SST, SSS, Chl-a, SLD, and the normal modes for the variables obtained from the EOF analyses. α are the coefficients for those predictors without a time lag and β are the coefficients for the predictors with a one-year lag. In this latter case, the sub-index starts at zero to account for the possibility of including the autoregressive term. In other words, the first term in the second summation of the right-hand side in Eq. (1) would be $\beta_0 S(t-1)$.

In this first analysis, the complete time series were used, that is, no trend was subtracted from either the sardine landings, or the predictor variables. The procedure for selecting the best approximating model was the following (Vargas-Yáñez et al., 2009): one year of the time series (both response and predictors) was suppressed. A multiple linear regression was applied to the remaining *n-1* data. A forward stepwise procedure was used and partial F values were calculated for each predictor at each step. A probability of $p = 0.05$ was used to enter a new predictor into the model, and $p = 0.1$ to remove it (see, for instance, Draper and Smith, 1981). Co-linearity between predictors was checked by means of the Variance Inflation Factor (VIF), which was below 3 for all the predictors and models considered. This procedure was repeated n times (each time different data was suppressed from the original time series). For each step, a different model was selected for the forward stepwise regression and this was considered a candidate model.

Finally, once a set of candidate models had been selected, a multiple linear regression was applied to each candidate model and for the complete time series (n data). The *AICc* (Corrected Akaike Information Criteria) were calculated according to Burnham and Anderson (2002). Finally, the candidate model with the minimum *AICc* was selected as the best approximating model. Fig. S1 in the supplementary material is a conceptual diagram explaining the procedure used for the model selection.

Once the final model had been selected, a cross-validation

procedure was applied (Francis, 2006; Lavín et al., 2007; Vargas-Yáñez et al., 2009). Using the selected model, landings for each year in the time series were estimated using the remaining *n-1* data, and the prediction was tested against the default estimate, which was considered to be the mean value of the time series (using the *n-1* data for the estimation). The reliability of the model can be tested by means of PVE (percent variance explained):

$$PVE = \frac{(MSE_{default} - MSE_{\mathrm{mod}\,el})}{MSE_{default}} \quad (2)$$

MSE is the mean squared error. Positive values for this statistic indicate that the model improves the default prediction.

Notice that in this first analysis, the series are not detrended and, therefore, the relationships between the response function (sardine landings) and predictors include possible relationships at both the inter-annual and long-term time scales.

2.3.3. Modeling detrended time series

In order to analyze the relationships between sardine landings and environmental variables on only an inter-annual time scale, the sardine landings and potential predictors (with and without time lag) were detrended. For instance, sardine landings were considered a linear trend, representing long-term changes, plus a term representing the inter-annual variability:

$$S(t) = \alpha_0 + \alpha_1 t + Z_S(t) \quad (3)$$

where *ZS* is the detrended time series and *a0* and *a1* are the intercept and slope, respectively. The detrended sardine landings were modeled as:

$$Z_S(t) = \sum_{i=1}^{k} \alpha'_i Z_i(t) + \sum_{j=0}^{k} \beta'_j Z_j(t-1) + \varepsilon(t) \quad (4)$$

That is, we used a multiple linear regression between the detrended sardine landings and the detrended potential predictors, with and without a one-year lag, and including a possible first-order autoregressive term. α' and β' are the regression coefficients. Primes are used to differentiate these from α and β in Eq. (1), as the coefficients from analyses using detrended and non- detrended time series will be different.

The procedure for selecting the best approximating model is the same as that explained in Section 2.3.2. *N* steps were followed. At each step, a data point was suppressed from the response function and the predictors and a forward stepwise multiple linear regression was used to fit a model, which is considered to be a candidate model. The candidate models were then used to model the complete time series (without suppressing any data), and the model with the minimum *AICc* was selected as the best approximating model.

2.3.4. Taking into account the linear trends

The analysis in Section 2.3.2 considers the fact that the possible relationship between the response function and the predictors is the same at both the long-term and inter-annual time scales. The analysis in Section 2.3.2 only considers the relationship between the sardine landings and the environmental variables at the inter-annual time scale. Nevertheless, in order to reconstruct the time series of sardine landings, both the linear trend and the inter-annual variability should be considered. Therefore the complete time series of sardine landings could be reconstructed as:

$$S(t) = a_0 + a_1 t + Z_S(t) = a_0 + a_1 t + \sum_{i=1}^{k} a'_i Z_i(t) + \sum_{j=0}^{k} \beta'_j Z_j(t-1) + \varepsilon(t) \quad (5)$$

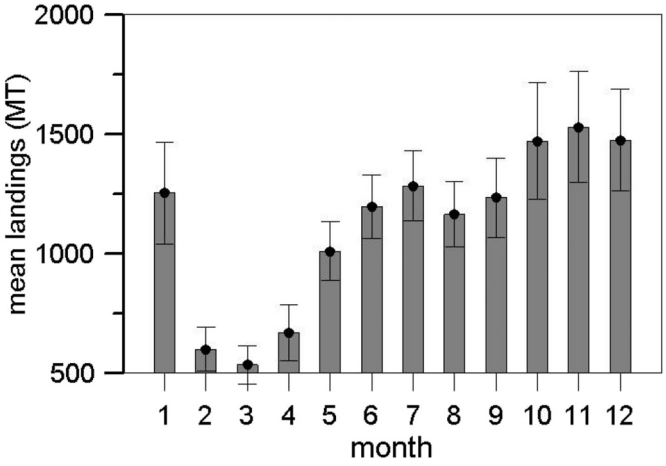

Fig. 3. Sardine landings averaged for each month of the year. The complete time series of sardine landings aggregated for the four Moroccan ports were used for the calculations. Vertical lines are the 95% confidence intervals for the mean values.

3. Results

The use of annually averaged time series avoids seasonal sardine landing patterns influencing our analyses. Nevertheless, there is clear seasonality, with minimum values during winter months (February to April) and an increase from spring to summer and autumn when maximum values are observed (Fig. 3).

The annual time series for SST, SSS, and Chl-a averaged for the southern Alboran Sea are presented in Fig. 4A, and the sea level difference (SLD) between Ceuta and Algeciras is shown in Fig. 4B. SST, SSS, and SLD show clear long-term trends, positive in the case of the temperature and salinity, and negative for SLD (Table 1). The available chlorophyll data start in 1997. This time series peaks in 2010,

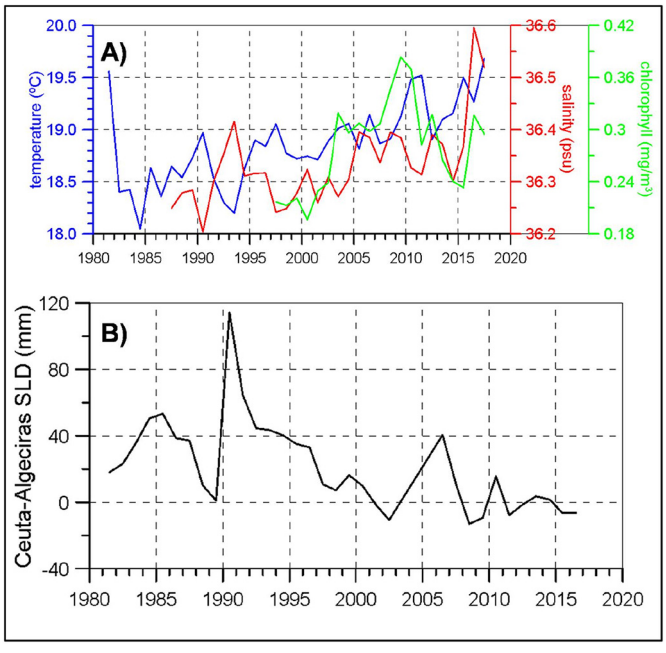

Fig. 4. A) Mean annual time series of SST (blue line), SSS (red line) and Chl-a (green line). These time series are obtained averaging SST, SSS and Chl-a data from the southern Alboran Sea (south of 36° N). B) Mean annual sea level difference between Ceuta and Algeciras expressed in mm. (For interpretation of the references to color in this figure legend, the reader is referred to the web version of this article.)

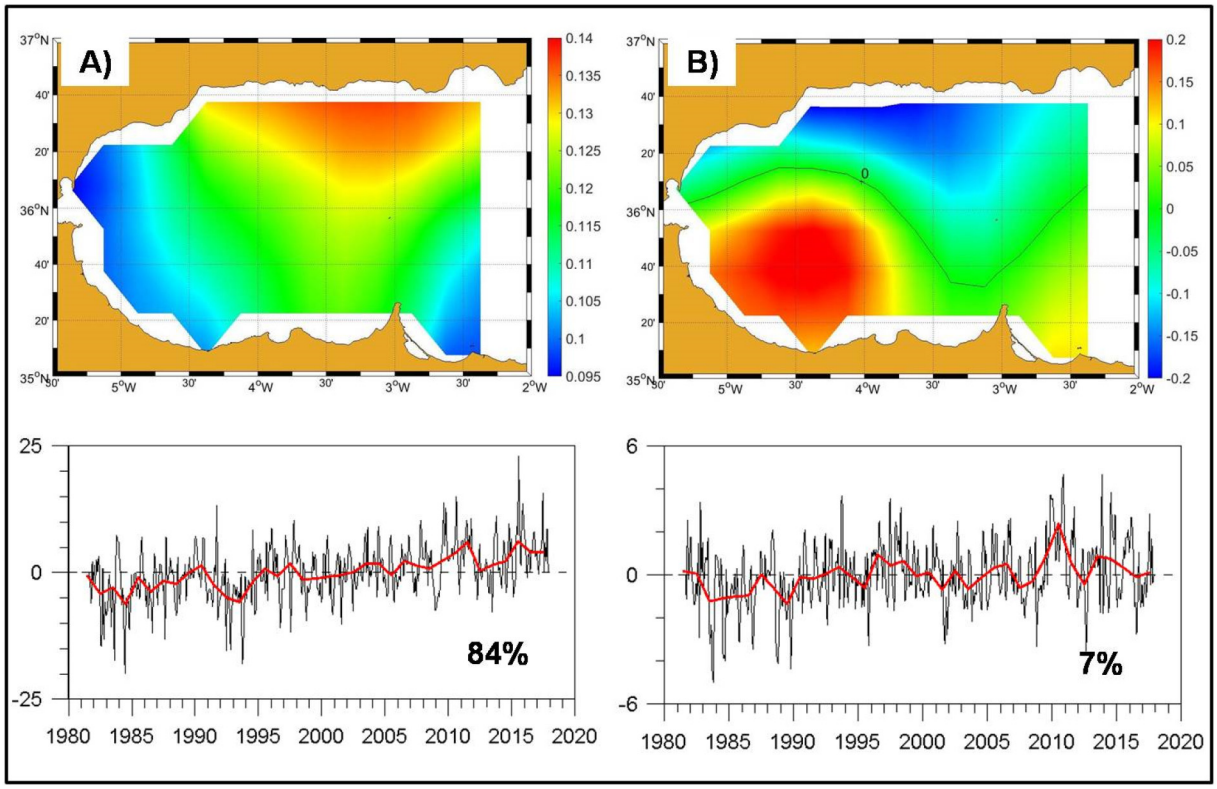

Fig. 5. Upper plots are the spatial weights for the two first SST EOFs. These weights are expressed by means of a color scale. A black continuous line is included to indicate the zero value. Notice that the first EOF has no sign change indicating an in phase variability in the whole basin. The second EOF shows the positive values in the southern half of the Alboran Sea and negative ones on the northern half, indicating an opposite variability on both halves. The lower panels are the time evolution or modes of variability corresponding to each EOF. The instantaneous SST change at any grid point is obtained multiplying the spatial weight in the upper panel times the instantaneous value of the corresponding time series (lower panel).

decreasing again towards 2016. The entire time series from 1997 to 2016 shows a net increase with a significant linear trend (Table 1). In contrast, the NAO index (both annual and winter values), and the MOI showed no significant trends during the analyzed period. The WeMO showed a significant negative trend from 1983 to 2016.

Fig. 5 shows the spatial weighting for the first two EOFs, corresponding to the SST and the time evolution of the corresponding modes of variability. Most of the variance is associated with the first mode (84%). The first four modes account for 97% of the total variance. The first EOF (spatial weights) has no sign change and represents an in-phase oscillation of the temperature over the whole basin. The time evolution of this mode of variability shows a positive trend, which simply reflects the current warming of the western Mediterranean. The second EOF reflects out-of-phase variability of the SST between the northern and southern Alboran Sea. When the time evolution of the associated mode is positive, the negative weights in the northern sector of the Alboran Sea indicate that SST values are below the climatological mean, while the southern half experiences positive (warming) anomalies.

Figs. 6 and 7 are similar to Fig. 5, presenting the first two EOFs and the time evolution of the variability modes for the SSS and Chl-a. The first four EOFs for SSS represent 84% of the total variance. The interpretation for the first and second EOFs and their time evolution is similar to that for the temperature. The first EOF represents the salinity variations, which occur with the same sign over the entire basin, and the positive trend for the mode indicates the salinity increase recently observed in the Mediterranean Sea. The second EOF reflects contrasting changes in the northern and southern sectors of the Alboran Sea. The third and fourth EOFs are not shown and are more difficult to interpret. They seem to be associated to changes in the direction of the Atlantic Jet flowing from the northern Alboran Sea towards Cape Tres Forcas, and to the upwelling region in the northwestern Alboran Sea.

The structure of the EOFs associated with the surface chlorophyll concentration is somehow more complex. The first four EOFs only account for 59% of the variance. Twelve modes were statistically significant, although those from EOF 5 accounted for low percentages of variance and showed difficult-to-interpret spatial patterns. The first and second EOFs are shown in Fig. 7. The first EOF reflects changes with the same sign over the whole basin. Nevertheless, the amplitude of these changes is much higher in the upwelling areas located along the northern coast of the Alboran Sea. The amplitude of the changes is also higher along the path usually followed by the AJ, surrounding the Western Alboran Gyre. The second EOF shows out-of-phase variability between the two main upwelling areas in the northern Alboran Sea, corresponding to the NW Alboran Sea, between Punta Europa and Punta Calaburras, and the cyclonic circulation area in front of Malaga Bay.

3.1. Model results

The initial correlation analysis between sardine landings and environmental variables, with and without a one-year time lag, allowed us to discard some of the potential predictors. It is interesting to note that winter NAO, annual NAO, and the Mediterranean Oscillation Index time series showed no significant correlations. A more local index, the Western Mediterranean Oscillation index, was also considered and no significant correlations with sardine landings were found. These variables were, therefore, rejected for the final model selection.

3.1.1. Results from the modeling of complete time series

In the first analysis, time series with no linear trends subtracted were used. Thirty tests were carried out for the model selection. For

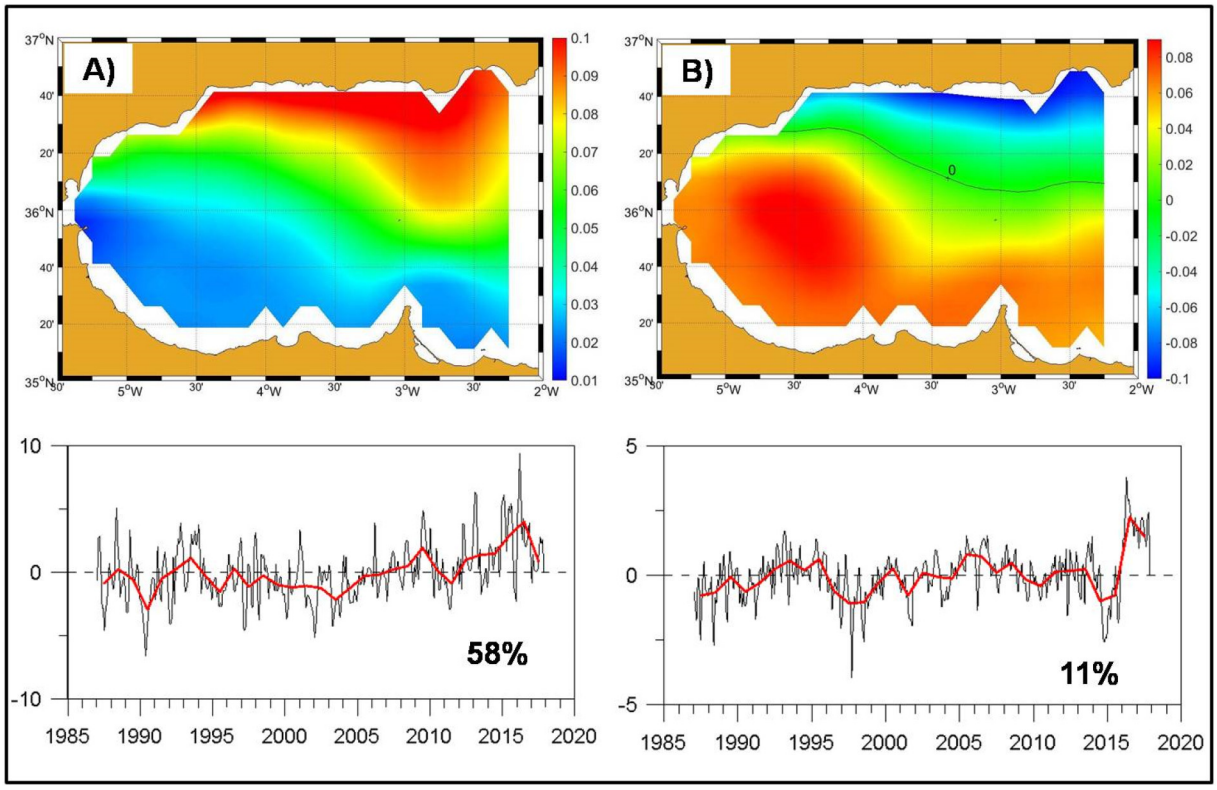

Fig. 6. The same as in Fig. 5, but for Sea Surface Salinity.

each test, a year was suppressed, and the linear model was selected by means of a forward stepwise multiple linear regression. The selected model was considered to be a candidate model. Note that Chl-a data are only available from 1997 onwards, therefore reducing the number of data points to 19. If the chlorophyll data are not considered, the time series involve 30 years, with SSS being the shortest series (1987–2016). Seven different models were selected. Most of the candidate models involved between one and three predictors. The seventh model selected

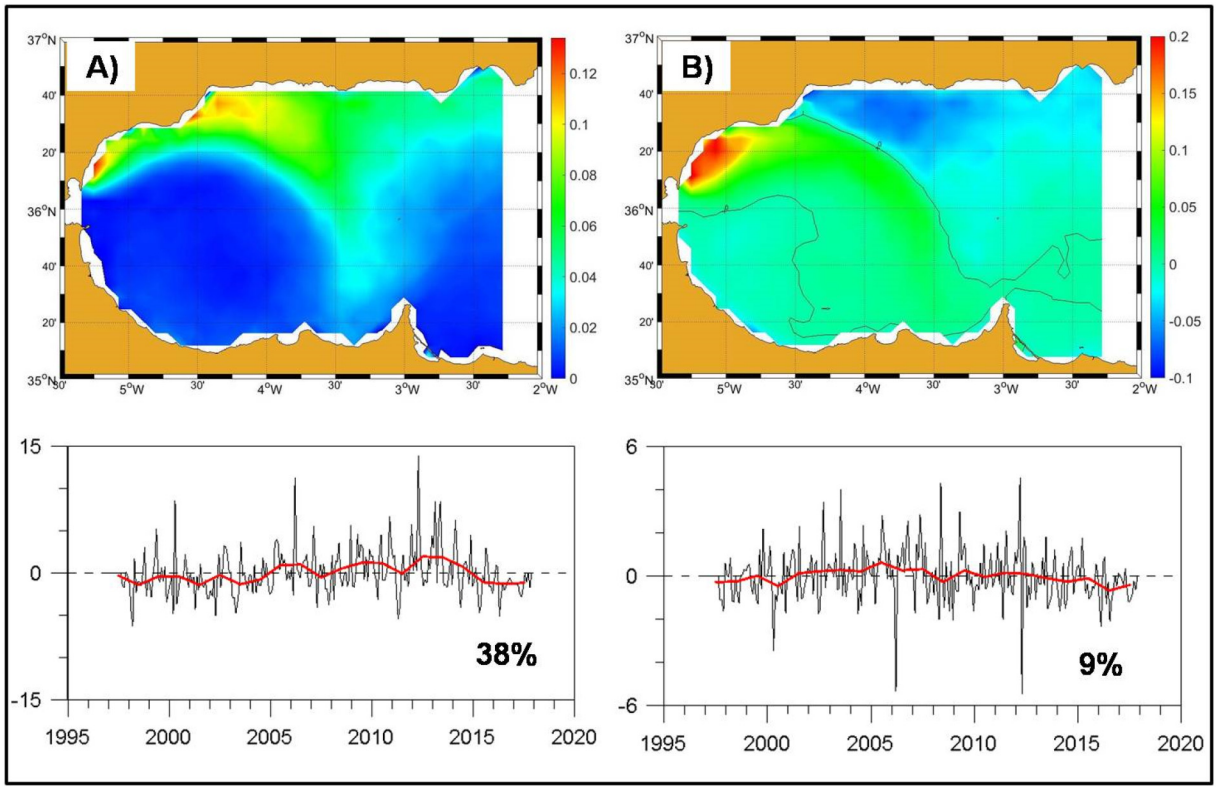

Fig. 7. The same as in Figs. 5 and 6, for surface Chlorophyll-a.

Table 2
Models selected and number of times each model was selected. Sardine landings were regressed on the environmental variables using a forward stepwise multiple linear regression. The process was repeated n times, suppressing a different year from the response and predictor variables each time. For each regression a different model was selected and it was considered as a candidate model. This table shows how many times each model was selected. Finally, the series containing all the years were used to calculate the AICc for each of the candidate models (last column). In this case the time series used were not detrended.

Model	SST (t-1)	U (t-1)	V (t)	Tmode1 (t-1)	Tmode1 (t)	Tmode2 (t-1)	Smode4 (t)	SLD (t)	Times	AICc
1	x						x	x	1	337.4
2					x			x	2	393.6
3				x				x	12	394.4
4	x							x	11	394.5
5				x	x			x	1	395.4
6	x					x		x	2	395.7

included six parameters (5 predictors and the ordinate intercept), but this was discarded as too many predictors (considering the length of the time series) could overfit the model. Table 2 shows the models selected and the times each model was selected.

Using the complete time series, the sardine landings were linearly regressed on each of the six candidate models. The Akaike Information Criterion, corrected for small samples (*AICc*), was calculated (column 11 in Table 2). According to the lowest *AICc* the model selected was:

$$S(t) = 10064.5 - 482.1SST(t-1) - 150.1S\,\mathrm{mode4}(t) + 7.3SLD(t) \quad (6)$$

The PVE statistic for this model was 50%. Fig. 8A shows the observed mean monthly landings (black line) and those predicted by the selected model (red line, model1 in Fig. 8A). The explained variance

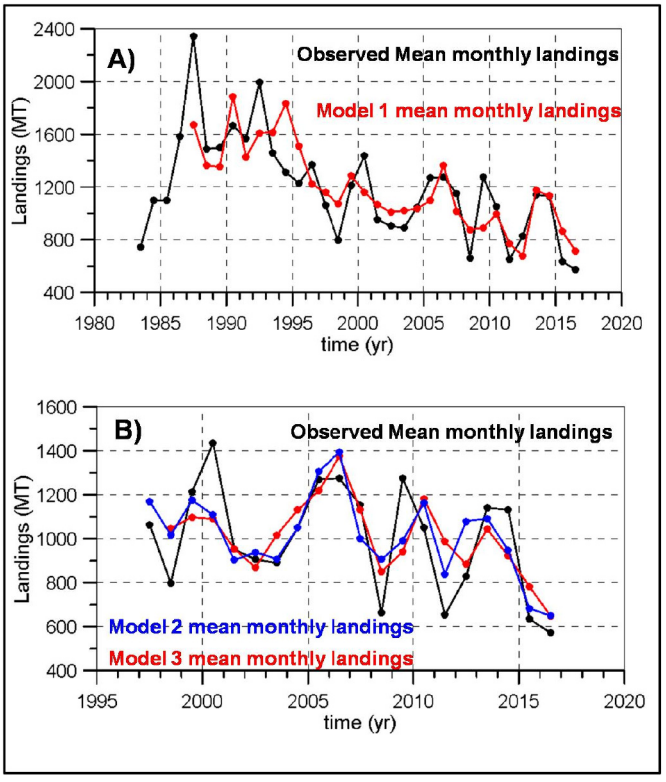

Fig. 8. A) Mean monthly landings: observed (black line) and predicted by model 1 (red line). Model 1 corresponds to the linear regression of sardine landings on environmental variables using the complete time series (without detrending). B) Mean monthly landings: observed (black line) and predicted by models 2 (blue line) and 3 (red line). Models 2 and 3 correspond to the linear regression of detrended sardine landings on detrended environmental variables and the addition of the linear trend for the time series of sardine landings (see Section 3.1.3. taking into account linear trends and Table 4 for the definition of the models). (For interpretation of the references to color in this figure legend, the reader is referred to the web version of this article.)

was 0.64 ($p < 0.01$).

The sardine landings had a significant and negative trend over the 34-year period covered by our observations. This trend accounts for 31% of the time series variance (Table 1). Two of the selected predictors also had significant trends. A positive one of 0.03 °C/year for the SST, and a negative one of −1.78 mm/year for SLD, indicating that the sea level difference between Ceuta and Algeciras was decreasing. Consequently, the warming surface waters and the weakening of the AJ could be linked to the decrease in sardine abundance.

3.1.2. Results from the modeling of the detrended time series

The detrended time series of sardine landings were modeled using the detrended potential predictors (SST, SSS, Chl-a, wind velocity (u, v), SLD, and the normal modes for the temperature, salinity and Chl-a). In this case, six candidate models were obtained. All the models involved one or two predictors. Table 3 shows the candidate models and the times each one was selected by the forward stepwise linear regression. Column seven is the *AICc* for each model. According to the lowest *AICc*, the selected model relating the sardine landing anomalies with those from the predictors can be expressed as:

$$Z_S(t) = 1838.2Z_{chla}(t-1) + 8Z_{SLD}(t) \quad (7)$$

Following the notation in Eqs. (3) and (4), Z_S represents the residuals, or detrended sardine landings, and Z_{chla} and Z_{SLD} are the detrended chl-a and *SLD* time series. The PVE for this model was 35%. The explained variance was 0.44 and $p = 0.01$.

The second model in Table 3 includes the first mode for *Chl-a* and the *SLD* as predictors. This model was selected 12 times (Table 3) and also had a low *AICc* (210). The resulting model for the detrended time series can be expressed as:

$$Z_S(t) = 102.5Z_{Chl\,\mathrm{mode}l}(t) + 7.6_{SLD}(t) \quad (8)$$

The variance explained is 0.5 ($p = 0.01$).

3.1.3. Taking into account the linear trends

Reconstructing the time series of sardine landings requires the consideration of both the linear trend present in this time series and the inter-annual variability modeled using the detrended environmental

Table 3
The same as in Table 2, but using detrended time series, that is, a linear trend was subtracted to the time series of sardine landings and to the environmental variables before the multiple regression was carried out.

Model	Chl-a (t-1)	Smode2 (t-1)	Chla mode1(t)	SLD (t)	Times	AICc
1	x			x	1	204
2			x	x	12	210
3		x	x		1	213
4			x		1	215
5		x			2	317
6				x	2	392

Table 4
First row is the model selected according to the AICc criterion when the complete time series were used. Column 2 shows the mathematical expression of the model. Columns 3 and 4 are the R2 and associated p value for the model and the fifth column is the AICc value. Rows 2 and 3 are the two models selected when the detrended times series were used. The final series of sardine landings is reconstructed adding the linear trend to the linear model obtained from the multiple regression. Columns 3, 4 and 5 are the R2, p and AICc values for each model.

Model	Model	R^2	p	AICc
1	$S(t) = 10064.5 - 482.1SST(t-1) - 150.1S \bmod e4(t) + 7.3SLD(t)$	0.64	0.00	337
2	$S(t) = 44232.6 - 21.5t + 1838.2Z_{Chla}(t-1) + 8Z_{(SLD)}(t)$	0.5	0.01	204
3	$S(t) = 44232.6 - 21.5t + 102.5Z_{Chlmodel}(t) + 7.6Z_{SLD}(t)$	0.6	0.003	210

time series. Using the linear trend in Table 1 and Eq. (7), the landings can be expressed as:

$$S(t) = 44232.6 - 21.5t + 1838.2Z_{Chla}(t-1) + 8Z_{SLD}(t) \quad (9)$$

The observed and estimated landings according to the model in Eq. (9) are presented in Fig. 8B as a blue line (model 2).The explained variance is 0.5 and $p = 0.01$ (see Table 4).

If the linear trend is added to the second model in Table 3, the sardine landings can be reconstructed as:

$$S(t) = 44232.6 - 21.5t + 102.5Z_{Chl\,mod\,el}(t) + 7.6Z_{SLD}(t) \quad (10)$$

The variance explained is 0.6 ($p = 0.003$). This model is labeled as model 3 in Fig. 8B (red line).

A summary of the finally selected models for the time series including trends, for the detrended time series, and for time series reconstructed using linear trends and detrended time series is presented in Table 4.

4. Discussion

Sardine landings in the Moroccan Mediterranean waters show strong inter-annual variability as evidenced by the large variance of mean monthly landings (red line, Fig. 2), which can fluctuate between 50 and > 2000 tons. Superimposed on this inter-annual variability, a negative trend can be observed. The slope of the straight line fitted to the mean monthly landings shows a decrease of −21.5 t/year (Table 1). This is a considerable decrease in sardine landings as it represents a reduction of 710 tons in monthly average landings over the entire period (1983–2016). Notice that the mean value for the mean monthly landings is 1188 t.

One factor possibly affecting the decline in fish catches is fishing pressure (Piroddi et al., 2017; Pinsky et al., 2011). Unfortunately, effort data (fishing days) is only available from 2009 onwards and only shows inter-annual oscillations. No conclusions can be extracted from such a short time series. If overfishing has played any role in the decrease in sardine landings, possible changes prior to 2009 should be considered. On the other hand, changes in environmental conditions can affect the body condition of adults and their recruitment success, these alterations being especially important in the case of small, fast-growing, and early-maturing species such as the sardine (Brosset et al., 2017; Tugores et al., 2011; Hidalgo et al., 2011; Perry et al., 2005). As we have already mentioned, temperature is a key factor in determining the spawning season, which could be altered by the warming of surface waters. As a consequence, there could be a mismatch between spawning and other factors affecting larval survival, such as primary production. In addition, the warming of sea water could also increase water column stratification, reducing the injection of nutrients to the photic layer and decreasing primary production and prey availability for both larvae and adults. Salinity is not expected to directly influence the condition of adults, the larval survival, or recruitment success. Nevertheless, it is an indirect indicator of the existence of frontal and upwelling areas within the Alboran Sea, which have been proved to enhance primary production both on the eastern side of Gibraltar and in the northwestern Alboran Sea (Reul et al., 2002, 2005). The analysis of temperature and salinity time series in the southern Alboran Sea revealed a clear increase in both the temperature and salinity of surface waters, at rates of 0.03 °C/year and 0.004 ups/year, respectively. This is not surprising as several studies have already revealed that the Mediterranean Sea has been undergoing a process of warming and salinity increase, at least since the mid-twentieth century, very likely forced by global climate change (Garcia-Martinez et al., 2018; Vargas-Yáñez et al., 2017; Skliris et al., 2012; Nikjaer, 2009). Although it has been hypothesized that a warmer and more stable water column could decrease primary production, this effect has not been observed in the Alboran Sea, at least during the period analyzed in this work. Chlorophyll-a concentrations increased at a rate of 0.005 mg m^{-3}/year. Two possible explanations are proposed for this trend. On the one hand, although the upper layer has warmed, increasing water column stability, the salinity has also increased, having the opposite effect. Changes in temperature and salinity could counterbalance, preventing primary production reduction linked to a more stable water column. On the other hand, primary production in the Alboran Sea may not be very dependent on winter mixing, which would be generally inhibited by greater stratification of the upper water column. Indeed, the high primary production of the Alboran Sea could be associated to other mechanisms, such as the internal tide mixing in the Strait of Gibraltar or the frontal areas and the cyclonic circulation in the northern part of the Alboran Sea. This nutrient- and chlorophyll-rich water would be advected southwards by the AJ surrounding the Alboran anticyclonic gyres (Oguz et al., 2014; Garcia-Gorriz and Carr, 2001; Ruiz et al., 2001), having a positive effect on prey availability for sardine larvae and adults.

It is interesting to note the strong and significant negative trend for the cross-strait SLD. This variable could be considered to be proportional to the velocity of the inflowing Atlantic Water (Vargas-Yáñez et al., 2002; García-Lafuente et al., 1998), which in turn could be related to the direction of the AJ within the Alboran Sea and the probability of a shift occurring, from anticyclonic gyre circulation to coastal mode circulation with the AJ flowing close to the Moroccan coast (Bormans and Garrett, 1989). The decreased velocity of the AJ could be caused by increased atmospheric pressure over the Western Mediterranean (Candela et al., 1989). The MOI showed no long-term changes, indicating that the atmospheric pressure gradient over the Mediterranean as a whole experienced no changes in the period 1981–2016. Nevertheless, the WeMO, which takes into the account the atmospheric pressure gradient within the Western Mediterranean, did experience a negative and significant trend. This trend is the result of a decrease in the pressure difference between the Gulf of Cadiz and the northern Italy, which hinders the entrance of the AJ through the Strait of Gibraltar, decreasing the SLD across the strait this zone. Another possibility for the negative trend of the cross-strait SLD is a weakening of the exchange between the Atlantic and the Mediterranean. This could be caused by the warming of the Mediterranean and a decrease in the deep water formation in this sea. Nevertheless, the salinity increase in the Mediterranean would once again counter-balance the temperature effect. At the present, we are unaware of any work evidencing such a weakening of the Atlantic-Mediterranean exchange, and the analysis of this issue is beyond the scope of this study.

Apart from the possible causes driving the observed long-term trends, there seems to be a relationship between these and the decrease

in sardine landings. When these trends are not eliminated from the sardine landing and environmental time series, the best linear model selected relates the sardine landings with the SST from the previous year, with the fourth mode of salinity, and with the SLD from the same year as the landings (no time lag). It is also worth highlighting the fact that there is a negative relationship between landings and SST, with a coefficient in the linear model (see results or Table 4) of −482 t/°C. Therefore, it could be considered that the positive warming trend is partially responsible for the negative trend observed in sardine landings. The relationship between landings and SLD is positive, with a coefficient of 7.3 t/mm, and it could be considered that the negative trend in SLD influences the negative trend in the sardine landings. The possibility of a link between small pelagic fish abundances and the kinetic energy of the inflowing AJ is not a new hypothesis. Ruiz et al. (2013) suggested that an AJ with a high kinetic energy would enhance primary production in the northern Alboran Sea, but would increase larval dispersion, having a negative impact on larval survival and the annual anchovy recruitment. The relationship between the AJ velocity and the sardine abundance in the southern part of the Alboran Sea is positive, with higher velocities associated to higher abundances and vice versa. This behavior is the opposite of that described by Ruiz et al. (2013) for the northern sector. The explanation could be that the AJ does not directly impinge on the southern Alboran coast, but after having recirculated around the Western Alboran Anticyclonic Gyre (see Fig. 1); therefore the effect of high kinetic energy on larval dispersion is considerably diminished. In contrast, high AJ velocities are associated to higher chlorophyll concentrations in the northern sector, which are eventually advected southwards by the AJ (Oguz et al., 2014; Garcia-Gorriz and Carr, 2001), having a potentially positive effect on the fertilization of the southern Alboran waters. Finally, the fourth salinity mode has a negative relationship with the sardine landings. Nevertheless, this relationship must be linked only to the inter-annual variability. Although the salinity, averaged for the region, has a positive trend, this variability mode shows no significant overall trend.

Besides the possible influence of long-term temperature and SLD changes on the decline of sardine landings, the selected linear model (Eq. (6) and Table 4) is able to reproduce both the long-term and inter-annual variability of sardine landings, explaining 64% of the observed variance (Fig. 8A). A second possibility considered in this work is the elimination of the linear trends from both the response and predictors. This approach is expressed by Eqs. (3) and (4), where the linear trend is determined by fitting a straight line to the time series of landings, and the residuals represent the inter-annual fluctuations around the linear behavior. This approach provides no explanation for the long-term decrease in sardine landings, and the models assess the influence of the inter-annual fluctuations in environmental variables. Two possible models were obtained. The model labeled 2 in Fig. 8B and Table 4 relates the landing residuals positively with the chlorophyll concentration with a one-year time lag (coefficient 1838 t/mg Chl-a m^{-3}), and positively with the SLD (coefficient 8 t/mm). In model 3 (Fig. 8B and Table 4) there is also a positive relationship between the landings and the first mode for chlorophyll and SLD (coefficients 102.5 t/mg Chl a m^{-3} and 7.6 t/mm, respectively). The first mode for chlorophyll reflects an in-phase chlorophyll change across the entire Alboran Sea. Therefore, both results (models 2 and 3) indicate that an increase in chlorophyll concentrations the year prior to, or during the year when the sardine catches are recorded, positively influences sardine abundance. Once again, the kinetic energy of the inflowing AJ seems to be an important factor. In all cases, the results obtained are very similar, with an increase/decrease of around eight tons for an increase/decrease of 1 mm in the cross-strait SLD. When the time series of landings is reconstructed using the estimated linear trend and the linear model for the residuals or detrended time series (Eqs. (9) and (10) and Table 4), the explained variance is 50% and 60% for models 2 and 3, respectively. The beneficial effect of increasing chlorophyll concentrations on the success of anchovy recruitment had already been reported for the northern Alboran Sea by Ruiz et al. (2013).Other authors have evidenced the fact that sardine larvae prey on phytoplankton and microzooplankton. Therefore, chlorophyll-rich waters would favor the survival of sardine larvae (Morote et al., 2010; Palomera et al., 2007). This not only affects sardines, but is also consistent with the strong survival-dependence of juvenile hakeoninter-annual chlorophyll variations (Hidalgo et al., in press).

In addition to the long-term and inter-annual variability of sardine landings, seasonal variability is also evidenced by the average landings calculated for each month of the year using the whole time series (Fig. 3). This seasonal cycle shows that minimum landings correspond to the February–April period. Mean temperatures for these months have also been calculated from the satellite data used in this study; these values range from 15.5 °C to 16.5 °C. Landing maximums are recorded from October to January. The autumn maximum landings are a clear and recurrent pattern, and it is very likely that this reflects the sardine annual recruitment, which is completed by September (Tugores et al., 2011). According to INRH (2015), the sardine breeding season is between January and March. It can be hypothesized that minimum landings correspond to the spawning season. Nevertheless, the temperature range shown in this data is slightly higher than the temperature range found by Bernal et al. (2007), who considered the spawning season to occur when the surface temperature was between 13.5 °C and 15 °C. The minimum landings also appear to occur later than the maximum Gonad Somatic Index found by Abad and Giráldez (1993) for the northern part of the Alboran Sea. These authors reported maximum values in December and January. From the present data, it could be concluded that the reproductive season in the southern part of the Alboran Sea is delayed with respect to the nearby Atlantic coast and the northern side of the Alboran Sea, or simply that the minimum landings correspond to the months after the spawning season and before the juveniles start to be recruited.

In summary, long-term sardine landings from 1981 to 2016 have experienced an important decrease in the southern Alboran Sea. Although the effect of increasing fishing pressure should be taken into account in future work, the present scarcity of fishing effort data does not allow us to draw any conclusions in regard to this issue. Linear models reflect the possible influence of Alboran Sea warming (likely linked to climate change), and a decrease in the kinetic energy of the AJ, on the observed decreasing trends in sardine landings. One of the expected effects of climate change involves increased water column stratification and weakened winter mixing, leading to less nutrient injection into the photic layer and lower intensity winter/spring phytoplankton blooms. To date, these changes have not been observed in the Alboran Sea, and the chlorophyll time series show a positive trend. A possible explanation for this is that the effect of warming waters on the water column stratification could be counterbalanced in the Mediterranean Sea by the opposite effect associated with the salinity increase. Another possibility is that the Alboran Sea is subject to specific upwelling mechanisms, such as frontal structures and cyclonic circulation areas. The chlorophyll concentration in surface waters seems to be an important factor modulating the variation in inter-annual sardine landings. Finally, linear models are capable of explaining around 60% of the landing variance, both for long-term and inter-annual variability.

Supplementary data to this article can be found online at https://doi.org/10.1016/j.jmarsys.2018.12.002.

Acknowledgements

This work has been partially funded by the project DILEMA CTM2014-59244-C3-2-R from the Spanish I+D+I national program. Ayman Jghab acknowledges an intern fellowship supported by the General Fisheries Commission for the Mediterranean, Food and Agriculture Organization of the United Nations.

References

Abad, R., Giráldez, A., 1993. Aspects on the reproductive biology of the western Mediterranean anchovy from the coasts of Malaga (Alboran Sea). Bol. Inst. Esp. Oceanogr. 8 (2), 145–155.

Abdellaoui, B., Berraho, A., Falcini, F., Jr, Santoleri, Sammartino, M., Pisano, A., Idrissi, M.H., Hilm, K., 2017. Assessing the impact of temperature and chlorophyll variations on the fluctuations of sardine abundance in Al-Hoceima (south Alboran Sea). J. Mar. Sci. 2017. https://doi.org/10.4172/2155-9910.1000239.

Albo-Puigserver, M., Muñoz, A., Navarro, J., Coll, M., Pethybridge, H., Sánchez, S., Palomera, I., 2017. Ecological energetics of forage fish from the Mediterranean Sea: seasonal dynamics and interspecific differences. In: Deep Sea Research Part II Topical Studies in Oceanography, https://doi.org/10.1016/j.dsr2.2017.03.002.

Bakun, A., 1996. Patterns in the ocean. In: Ocean Processes and Marine Population Dynamics. California Dea Grant College System, C.A. (323 pp).

Baldacci, A., Corsini, G., Grasso, R., Manzella, G., Allen, J.T., Cipollini, P., Guymer, T.H., Snaith, H.M., 2001. A study of the Alboran sea mesoscale system by means of empirical orthogonal function decomposition of satellite data. J. Mar. Syst. 29 (1–4), 293–311.

Barroeta, Legarreta, Z., Olivar, M., Palomera, I., 2017. Energy density of zooplankton and fish larvae in the southern Catalan Sea (NW Mediterranean). J. Sea Res. 124. https://doi.org/10.1016/j.seares.2017.04.008.

Bernal, M., Stratoudakis, Y., Coombs, S., Angelico, M.M., Lago De Lanzós, A., Porteiro, C., Sagarminaga, Y., Santos, M., Uriarte, A., Cunha, E., 2007. Sardine spawning off the European Atlantic coast: characterization of and spatio-temporal variability in spawning habitat. Prog. Oceanogr. 74 (2–3), 210–227.

Bethoux, J.P., Gentili, B., Morin, P., Nicolas, E., Pierre, C., Ruiz-Pino, D., 1999. The Mediterranean Sea: a miniature ocean for climatic and environmental studies and a key for the climatic functioning of the North Atlantic. Prog. Oceanogr. 44, 131–146.

Bormans, M., Garrett, C., 1989. A simple criterion for gyre formation by the surface outflow from a striat, with aplication to the Alboran Sea. J. Geophys. Res. 94 (C9), 12637–12644.

Bosc, E., Bricaud, A., Antoine, D., 2004. Seasonal and inter-annual variability in algal biomass and primary production in the Mediterranean Sea, as derived from 4 years of SeaWiFS observations. Glob. Biogeochem. Cycles 18, GB1005. https://doi.org/10.1029/2003GB002034.

Brosset, P., Ménard, F., Fromentin, J.-M., Bonhommeau, S., Ulses, C., Bourdeix, J.-H., Bigot, J.-L., Van Beveren, E., Roos, D., Saraux, C., 2015. Influence of environmental variability and age on the body condition of small pelagic fish in the Gulf of Lions. Mar. Ecol. Prog. Ser. 529, 219–231. https://doi.org/10.3354/meps11275.

Brosset, P., Le Bourg, B., Costalago, D., Banaru, D., Van Beveren, E., Bourdeix, J.-H., Fromentin, J.-M., Ménard, F., Sarux, C., 2016. Linking small pelagic dietary shifts with ecosystem changes in the Gulf of Lions. Mar. Ecol. Prog. Ser. 554, 157–171. https://doi.org/10.3354/meps11796.

Brosset, P., Fromentin, J.-M., Van Beveren, E., Lloret, J., Marques, V., Basilone, G., Bonanno d, A., Carpi, Piera, Donato, F., CikeškKec, V., De Felice, A., Ferreri, R., Gašparevic´, D., Giráldez, A., Gücü, A., Iglesias, M., Leonori, I., Palomera, I., Somarakis, S., Tic˘ina, V., Torres, P., Ventero, A., Zorica, B., Ménardm, F., Saraux, C., 2017. Spatio-temporal patterns and environmental controls of small pelagic fish body condition from contrasted Mediterranean areas. Prog. Oceanogr. 151, 149–162. https://doi.org/10.1016/j.pocean.2016.12.002.

Burnham, K.P., Anderson, D.R., 2002. Model Selection and Multimodel Inference: A Practical Information-Theoretic Approach, 2nd edition. Springer-Verlag, New York, NY, USA (488 pp).

Candela, J., Winant, C.D., Bryden, H.L., 1989. Meteorologically forced subinertial flows through the Strait of Gibraltar. J. Geophys. Res. 94 (C9), 12667–12679.

Coll, M., Piroddi, C., Albouy, C., RaisLasram, F.B., Cheung, W.W.L., Christensen, V., Karpouzi, V.S., Guilhaumon, F., Mouillot, D., Paleczny, M., Palomares, M.L., Steenbeek, J., Trujillo, P., Watson, R., Pauly, D., 2011. The Mediterranean Sea under siege: spatial overlap between marine biodiversity, cumulative threats and marine reserves. Glob. Ecol. Biogeogr. https://doi.org/10.1111/j.1466-8238.2011.00697.x.

CopeMed II, 2017. Report of the 6th Meeting of CopeMed II Study Group on Demersal and Small Pelagic Stocks of Interest to Algeria, Morocco and Spain in the Alboran Sea (GSAs 01, 02, 03 and 04). Malaga, Spain 9–11 October 2017. 2017 CopeMed II Technical Documents N°48 (GCP/INT/028/SPA - GCP/INT/006/EC), Malaga (42pp).

Costalago, D., Navarro, J., Álvarez-Calleja, I., Palomera, I., 2012. Ontogenetic and seasonal changes in the feeding habits and trophic levels of two small pelagic fish species. Mar. Ecol. Prog. Ser. 460 (julio), 169–181. https://doi.org/10.3354/meps09751.

Costalago, D., Palomera, I., Tirelli, V., 2014. Seasonal comparison of the diets of juvenile European anchovy *Engraulis encrasicolus* and sardine *Sardina pilchardus* in the Gulf of Lions. J. Sea Res. 89 (mayo), 64–72. https://doi.org/10.1016/j.seares.2014.02.008.

Draper, N.R., Smith, H., 1981. Applied Regression Analysis, 2nd ed. Wiley, New York.

FAO, 2008. FAO fisheries report no. 870. In: FAO Expert Workshop on Climate Change Implications for Fisheries and Aquiculture, (Rome, 7–9 April 2008).

FAO, 2011. Review of the world marine fishery resources. In: FAO Fisheries and Aquiculture Technical Report No. 569. FAO, Rome (334 pp).

FAO, 2016. The State of Mediterranean and Black Sea Fisheries. General Fisheries Commission for the Mediterranean, Rome 134 pp. also available at. http://www.fao.org/3/a-i5496e.pdf.

Fernández de Puelles, M., Alemany, F., Jansá, J., 2007. Zooplankton time-series in the Balearic Sea (Western Mediterranean): variability during the decade 1994–2003. Prog. Oceanogr. 74, 329–354. https://doi.org/10.1016/j.pocean.2007.04.009.

Francis, R.I.C., 2006. Measuring the strength of environmental–recruitment relationships: the importance of including predictor screening with cross-validation. ICES J. Mar. Sci. 63, 594–599. https://doi.org/10.1016/j.icesjms.2006.01.001.

García-Comas, C., Stemmann, L., Ibáñez, F., Berline, L., GraziaMazzocchi, M., Gasparini, S., Picheral, M., Gorsky, G., 2011. Zooplankton long-term changes in the NW Mediterranean Sea: decadal periodicity forced by winter hydrographic conditions related to large-scale atmospheric forcing. J. Mar. Syst. 87, 216–226. https://doi.org/10.1016/j.marsys.2011.04.003.

Garcia-Gorriz, E., Carr, M.E., 2001. Physical control of phytoplankton distributions in the Alboran Sea: a numerical and satellite approach. J. Geophys. Res. 106, 16795–16806. https://doi.org/10.1029/1999JC000029.

García-Lafuente, J., Cano, N., Vargas-Yáñez, M., Rubín, J.P., Hernández-Guerra, A., 1998. Evolution of the Alboran Sea hydrographic structures during July 1993. Deep-Sea Res. I 45, 39–65.

Garcia-Martinez, M.C., Vargas-Yañez, M., Moya, F., Zunino, P., Bautista, B., 2018. The effects of climate change and rivers damming in the Mediterranean sea during the twentieth century. Int. J. Environ. Sci. Nat. Res. 8 (4). https://doi.org/10.19080/IJESNR.2018.08.555741.

GFCM, 2016. Final Report of the Working Group on Stock Assessment of Small Pelagic Species (WGSASP).

Guisande, C., Vergara, A.R., Riveiro, I., Cabanas, J.M., 2004. Climate change and abundance of the Atlantic-Iberian sardine (*Sardina pilchardus*). Fish. Oceanogr. 13 (2), 91–101.

Hidalgo, M., Rouyer, T., Molinero, J.C., Massutí, E., Moranta, J., Guijarro, B., Stenseth, N.Chr., 2011. Synergistic effects of fishing-induced demographic changes and climate variation on fish population dynamics. Mar. Ecol. Prog. Ser. 426, 1–12. https://doi.org/10.3354/meps09077.

Hidalgo, M., Rueda, L., Molinero, J.C., Guijarro, B., Massutí, E., 2015. Spatial and temporal variation of seasonal synchrony in the deep-sea shrimp *Aristeus antennatus* in the Western Mediterranean. J. Mar. Syst. 148, 131–141. https://doi.org/10.1016/j.jmarsys.2015.02.007.

Hidalgo, M., Ligas, A., Bellido, J.M., Bitetto, I., Carbonara, P., Carlucci, R., Guijarro, B., Jadaud, A., Lembo, G., Manfredi, C., Esteban, A., Garofalo, G., Ikica, Z., García, C., Gil de Sola, L., Kavadas, S., Maina, I., Sion, L., Vittori, S., Vrgoc, N., 2018. Size-dependent survival 2 of European hake juveniles in the Mediterranean Sea. Sci. Mar (in press).

INRH/DRH, 2015. Rapport Annuel de l'Etat des Stocks et des Pêcheriesmarocaines 2015. (295 pp).

INRH/DRH, 2016. Rapport Annuel de l'etat des Stocks et des Pêcheriesmarocaines 2016. (294 pp).

Kalnay, E., Kanamitsu, M., Kistler, R., Collins, W., Deaven, D., Gandin, L., Iredell, M., Saha, S., White, G., Woollen, J., Zhu, Y., Leetmaa, A., Reynolds, R., Chelliah, M., Ebisuzaki, W., Higgins, W., Janowiak, J., Mo, K.C., Ropelewski, C., Wang, J., Jenne, Roy, Joseph, Dennis, 1996. The CEP/NCAR 40-year reanalysis project. Bull. Am. Meteorol. Soc. 77, 437–470.

Lavín, A., Montero-Ventas, X., Ortiz De Zárate, V., Abaunza, P., Cabanas, J.M., 2007. Environmental variability in the North Atlantic and Iberian waters and its influence on horse mackerel (*Trachurus trachurus*) and albacore (*Thunnus alalunga*) dynamics. ICES J. Mar. Sci. 64 (3), 425–438. https://doi.org/10.1093/icesjms/fsl042.

Lloret, J., Palomera, I., Salat, J., Sole, I., 2004. Impact of freshwater input and wind on landings of anchovy (*Engraulis encrasicolus*) and sardine (*Sardina pilchardus*) in shelf waters surrounding the Ebre (Ebro) River delta (north-western Mediterranean). Fish. Oceanogr. 13 (2), 102–110.

Martín-Bide, J., López-Bustins, J.A., 2006. The Western Mediterranean oscillation and rainfall in the Iberian Peninsula. Int. J. Climatol. 26, 1455–1475.

Massutí, E., Monserrat, S., Oliver, P., Moranta, J., López-Jurado, J.L., Marcos, M., Hidalgo, M., Guijarro, B., Carbonell, A., Pereda, P., 2008. The influence of oceanographic scenarios on the population dynamics of demersal resources in the western Mediterranean: hypothesis for hake and red shrimp off Balearic Islands. J. Mar. Syst. 71, 421–438. https://doi.org/10.1016/j.jmarsys.2007.01.009.

Minas, H.J., Coste, B., Le Corre, P., Minas, M., Raimbault, P., 1991. Biological and geochemical signatures associated with the water circulation through the Strait of Gibraltar and in the western Alboran Sea. J. Geophys. Res. 96 (C5), 8755–8771. https://doi.org/10.1029/91JC00360.

Morán, X.A.G., Estrada, M., 2001. Short-term variability of photosynthetic parameters and particulate and dissolved primary production in the Alboran Sea (SW Mediterranean). Mar. Ecol. Prog. Ser. 212, 53–67.

Morote, E., Olivar, M., Villate, F., Uriarte, I., 2010. A comparison of anchovy (*Engraulis encrasicolus*) and sardine (*Sardina pilchardus*) larvae feeding in the Northwest Mediterranean: influence of prey availability and ontogeny. ICES J. Mar. Sci. 67, 897–908. https://doi.org/10.1093/icesjms/fsp302.

National Centre for Atmospheric Research, 2017. In: Hurrell, James, National Center for Atmospheric Research Staff (Eds.), The Climate Data Guide: Hurrell North Atlantic Oscillation (NAO) Index (Station-Based), Last modified 07 Nov 2017. Retrieved from. https://climatedataguide.ucar.edu/climate-data/hurrell-north-atlantic-oscillation-nao-index-station-based.

Nikjaer, L., 2009. Mediterranean Sea surface warming 1985–2006. Clim. Res. 39, 11–17. https://doi.org/10.3354/cr00794.

Oguz, T., Macias, D., Garcia-Lafuente, J., Pascual, A., Tintore, J., 2014. Fueling plankton production by a meandering frontal jet: a case study for the Alboran Sea (Western Mediterranean). PLoS One 9 (11), e111482. https://doi.org/10.1371/journal.pone.0111482.

Olivar, M.P., Salat, J., Palomera, I., 2001. Comparative study of spatial distribution patterns of the early stages of anchovy and pilchard in the NW Mediterranean Sea. Mar. Ecol. Prog. Ser. 217, 111–120. https://doi.org/10.3354/meps217111.

Olivar, M., Emelianov, M., Villate, F., Uriarte, I., Maynou, F., Álvarez, I., Morote, E., 2010. The role of oceanographic conditions and plankton availability in larval fish assemblages off the Catalan coast (NW Mediterranean). Fish. Oceanogr. 19, 209–229. https://doi.org/10.1111/j.1365-2419.2010.00538.x.

Palomera, I., Olivar, M.P., Salat, J., Sabatés, A., Coll, M., García, A., Morales-Nin, B., 2007. Small pelagic fish in the NW Mediterranean Sea: an ecological review. Prog. Oceanogr. 74, 377–396. https://doi.org/10.1016/j.pocean.2007.04.012.

Parada, M., Canton, M., 1998. The spatial and temporal evolution of thermal structures in the Alboran Sea Mediterranean basin. Int. J. Remote Sens. 19 (11), 2119–2131. https://doi.org/10.1080/014311698214901.

Perry, A.L., Low, P.J., Ellis, J.R., Reynolds, J.D., 2005. Climate change and distribution shifts in marine fishes. Science 308, 1912–1915.

Pinsky, M.L., Jensen, O.P., Ricard, D., Palumbia, S.R., 2011. Unexpected patterns of fisheries collapse in the world's oceans. Proc. Natl. Acad. Sci. U. S. A. 108 (20), 8317–8322. https://doi.org/10.1073/pnas.1015313108.

Piroddi, C., Coll, M., Liquete, C., Macías, D., Greer, K., Buszowski, J., Steenbeek, J., Danovaro, R., Christensen, V., 2017. Historical changes of the Mediterranean Sea ecosystem: modeling the role and impact of primary productivity and fisheries changes over time. Sci. Rep. 7, 44491. https://doi.org/10.1038/srep44491.

Preisendorfer, R.W., 1988. In: Mobley, C.D. (Ed.), Principal Component Analysis in Meteorology and Oceanography. Elsevier, Amsterdam (425 pp).

Raybaud, V., Bacha, M., Amara, R., Beaugrandd, G., 2017. Forecasting climate-driven changes in the geographical range of the European anchovy (*Engraulis encrasicolus*). ICES J. Mar. Sci. 74 (5), 1288–1299. https://doi.org/10.1093/icesjms/fsx003.

Reul, A., Vargas, J.M., Jiménez-Gómez, F., Echevarría, F., García-Lafuente, J., Rodríguez, J., 2002. Exchange of planktonic biomass through the Strait of Gibraltar in late summer conditions. Deep-Sea Res. II 49, 4131–4144.

Reul, A., Rodríguez, V., Jiménez-Gómez, F., Blanco, J.M., Bautista, B., Sarhan, T., Guerrero, F., Ruiz, J., García-Lafuente, J., 2005. Variability in the spatio-temporal distribution and size-structure of phytoplankton across an upwelling area in the NW-Alboran Sea (W-Mediterranean). Cont. Shelf Res. 25 (5–6), 589–608.

Reynolds, Richard W., Smith, Thomas M., Liu, Chunying, Chelton, Dudley B., Casey, Kenneth S., Schlax, Michael G., 2007. Daily high-resolution-blended analyses for sea surface temperature. J. Clim. 20, 5473–5496.

Ruiz, J., Echevarría, F., Font, J., Ruiz, S., García, E., Blanco, J.M., Jiménez-Gómez, F., Prieto, L., González-Alaminos, A., García, C.M., Cipollini, P., Snaith, H., Bartual, A., Reul, A., Rodríguez, V., 2001. Surface distribution of chlorophyll, particles and gelbstoff in the Atlantic jet of the Alborán Sea: from submesoscale to subinertial scales of variability. J. Mar. Syst. 29 (1–4), 277–292.

Ruiz, Javier, Macías, Diego, Rincón, Margarita M., Pascual, Ananda, Catalán, Ignacio A., Navarro, G., 2013. Recruiting at the edge: kinetic energy inhibits anchovy populations in the Western Mediterranean. PLoS One 8 (2), e55523. https://doi.org/10.1371/journal.pone.0055523.

Sabatés, A., 2004. Diel vertical distribution of fish larvae during the winter-mixing period in the north western Mediterranean. ICES J. Mar. Sci. 61 (8), 1243–1252.

Sabatés, A., Martín, P., Lloret, J., Raya, V., 2006. Sea warming and fish distribution: the case of the small pelagic fish, *Sardinella aurita*, in the western Mediterranean. Glob. Chang. Biol. 12, 2209–2219. https://doi.org/10.1111/j.1365-2486.2006.01246.x.

Sabatés, A., Salat, J., Raya, V., Emelianov, M., Segura-Noguera, M., 2009. Spawning environmental conditions of *Sardinella aurita* at the northern limit of its distribution range, the western Mediterranean. Mar. Ecol. Prog. Ser. 385, 227–236. https://doi.org/10.3354/meps08058.

Sarhan, T., Lafuente, J.G., Vargas-Yáñez, M., Vargas, J.M., Plaza, F., 2000. Upwelling mechanisms in the northwestern Alboran Sea. J. Mar. Syst. 23 (4), 317–331.

Simoncelli, S., Fratianni, C., Pinardi, N., Grandi, A., Drudi, M., Oddo, P., Dobricic, S., 2014. Mediterranean Sea Physical Reanalysis (MEDREA 1987–2015) (Version 1) (set). E.U. Copernicus Marine Service Informationhttps://doi.org/10.25423/medsea_reanalysis_phys_006_004.

Skliris, N., Sofianos, S.S., Gkanasos, A., Mantziafou, A., Versatis, V., Axaopoulos, P., Lascaratos, A., 2012. Decadal scale variability of sea surface temperature in the Mediterranean Sea in relation to atmospheric variability. Ocean Dyn. https://doi.org/10.1007/s10236-011-0493-5.

Thiaw, M., Auger, P.-A., Ngom, F., Brochier, T., Faye, S., Diankha, O., Brehmer, P., 2017. Effect of environmental conditions on the seasonal and inter-annual variability of small pelagic fish abundance off North-West Africa: the case of both *Senegalese sardinella*. Fish. Oceanogr. 26, 583–601. https://doi.org/10.1111/fog.12218.

Tugores, M.P., Giannoulaki, M., Iglesias, M., Bonanno, A., Ticina, V., Leonori, I., Machias, A., Tsagarakis, K., Díaz, N., Giráldez, A., Patti, B., De Felice, A., Basilone, G., Valavanis, V., 2011. Habitat suitability modelling for sardine *Sardina pilchardus* in a highly diverse ecosystem: the Mediterranean Sea. Mar. Ecol. Prog. Ser. 443, 181–205. https://doi.org/10.3354/meps09366.

Vargas-Yáñez, M., Plaza, F., García-Lafuente, J., sarhan, T., Vargas, J.M., Vélez-belchi, P., 2002. About the seasonal variability of the Alboran Sea circulation. J. Mar. Syst. 35, 229–248.

Vargas-Yáñez, M., Moya, F., García-Martínez, M., Rey, J., González, M., Zunino, P., 2009. Relationships between *Octopus vulgaris* landings and environmental factors in the northern Alboran Sea (Southwestern Mediterranean). Fish. Res. 99, 159–167.

Vargas-Yáñez, M., García-Martínez, M.C., Moya, F., Balbín, R., López-Jurado, J.L., Serra, M., Zunino, P., Pascual, J., Salat, J., 2017. Updating temperature and salinity mean values and trends in the Western Mediterranean: the RADMED project. Prog. Oceanogr. 157, 27–46. https://doi.org/10.1016/j.pocean.2017.09.004.

Volpe, G., Colella, S., Forneris, V., Tronconi, C., Santoleri, R., 2012. The Mediterranean ocean colour observing system-system development and product validation. Ocean Sci. 8 (5), 869.

Zar, J.H., 1984. Biostatistical Analysis, 2nd edition. Prentice-Hall, Inc., Englewood Cliffs (718 p).